Optimization of Mo-Si-B Intermetallics

Joachim H. Schneibel and Peter F. Tortorelli
Metals and Ceramics Division, Oak Ridge National Laboratory, Oak Ridge, TN 37831, U.S.A
Matthew J. Kramer and Andrew J. Thom
Iowa State University, Ames Laboratory, Ames, Iowa 50011-3020, U.S.A.
Jamie J. Kruzic and Robert O. Ritchie
Materials Sciences Division, Lawrence Berkeley National Laboratory, and Department of Materials Science and Engineering, University of California, Berkeley, CA 94720, U.S.A.

ABSTRACT

Mo-Si-B intermetallics consisting of the phases Mo_3Si, Mo_5SiB_2, and α-Mo (Mo solid solution) can be designed to exhibit some degree of oxidation resistance, fracture toughness, and creep strength, but not necessarily all of these at the same time. For example, microstructures that enhance the oxidation resistance are typically associated with low fracture toughness. Examples will be given illustrating the oxidation resistance, fracture toughness, and creep strength of Mo-Si-B intermetallics as a function of their phase volume fractions as well as the topology and length scale of their microstructures. Microstructures containing either individual α-Mo particles or a continuous α-Mo matrix will be described. The examples provide possible ways to control the composition and microstructure of Mo-Si-B alloys such as to optimize the desired balance of properties.

INTRODUCTION

The Mo-Si-B ternary phase diagram exhibits two regions that have been of interest for several years. One region, which was the subject of pioneering research by Akinc and collaborators [1], consists of Mo_5Si_3, the T2 phase Mo_5SiB_2, and the A15 phase Mo_3Si, as shown in the light-gray triangle in Fig. 1. Alloys in this region of the phase diagram exhibit excellent oxidation resistance at elevated temperatures, e.g., 1300°C. Without the boron additions, much higher silicon concentrations, such as in $MoSi_2$, would be required [2,3]. The other alloying region, which is the subject of this paper, follows from the work of Berczik et al. [4,5]. It consists of the phases α-Mo, Mo_3Si, and T2 (see dark gray triangle in Fig. 1). While alloys containing a Mo solid solution phase are not as oxidation resistant as Mo_5Si_3-T2-Mo_3Si alloys, they exhibit a higher fracture toughness. The fracture toughness tends to increase with an increasing volume fraction of α-Mo and, for a given fraction, will be higher if the α-Mo forms as a continuous matrix instead of individual particles [6]. Since the creep strength of α-Mo is lower than that of Mo_3Si and T2, the creep strength of these alloys will depend on their α-Mo volume fraction. It should also depend on the topology of the microstructure. For example, if the α-Mo is distributed as a continuous matrix or "binder" phase instead of isolated particles, the creep strength should be relatively low.

EXPERIMENTAL DETAILS

There are several options for processing Mo-Si-B alloys. The first approach involves arc-melting elemental materials in argon followed by drop casting into a water-cooled copper crucible [7]. If the α-Mo volume fraction is less than 40 vol.% the ingots usually show macrocracks. This technique is therefore not suitable for alloys with low α-Mo volume fractions.

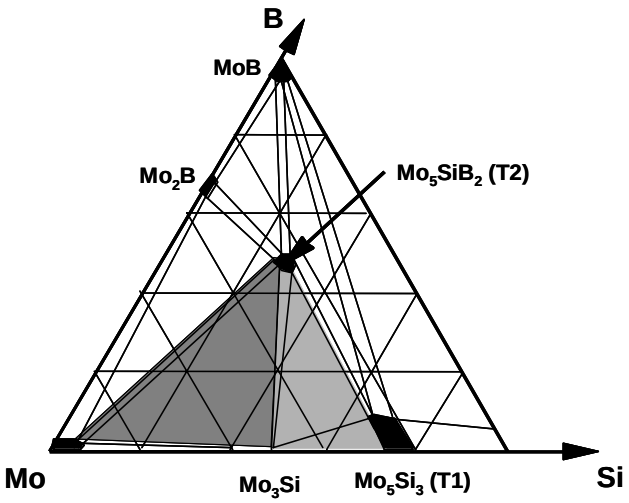

Figure 1. Schematic section of the Mo-Si-B ternary phase diagram [1].

The second approach consists of arc-melting followed by grinding to particle sizes ≤ 20 μm and sintering in high-purity argon at 1900°C [1]. The third approach involves hot isostatic pressing (HIPing) of pre-alloyed powders sealed in an evacuated Nb can [8]. For HIPing, the particle size can be much larger than that for free sintering. By vacuum-annealing the powders prior to HIPing, a Mo-rich shell can be formed on the powder surfaces. Consolidation then results in a material with a continuous α-Mo "binder" phase [8].

The high-temperature oxidation resistance of the alloys was qualitatively assessed under thermal cycling conditions. Specimens were held at temperature for a fixed period of time in air and then cooled to room temperature prior to subsequent identical cycles. In this paper, specimen mass changes are reported for a given number of cycles and are used as an indicator of oxidation resistance [9]. The procedure used for the fracture toughness measurements can be found in Choe et al. [10,11]. The creep strength was assessed by constant displacement rate compression testing in an argon atmosphere with an initial strain rate of 10^{-5} s^{-1} [12]. The creep strength was defined as the flow stress at a plastic strain of 2%, for which a reasonably constant flow stress indicating steady-state creep was usually established.

EXPERIMENTAL RESULTS AND DISCUSSION

Microstructures

Figure 2 shows typical microstructures for (a) cast and annealed, (b) sintered, and (c) HIPed Mo-Si-B alloys (note the differences in magnification). The α-Mo in the cast and annealed alloy appears to be discontinuous (Fig. 2a). The sintered microstructure in Fig. 2b also tends to contain discontinuous α-Mo particles, but does not contain the large primary α-Mo seen in Fig. 2a. The HIPed alloy contains a continuous α-Mo matrix phase. Using these microstructures as examples, the influence of the microstructure on oxidation resistance, fracture toughness, and creep strength is qualitatively discussed below.

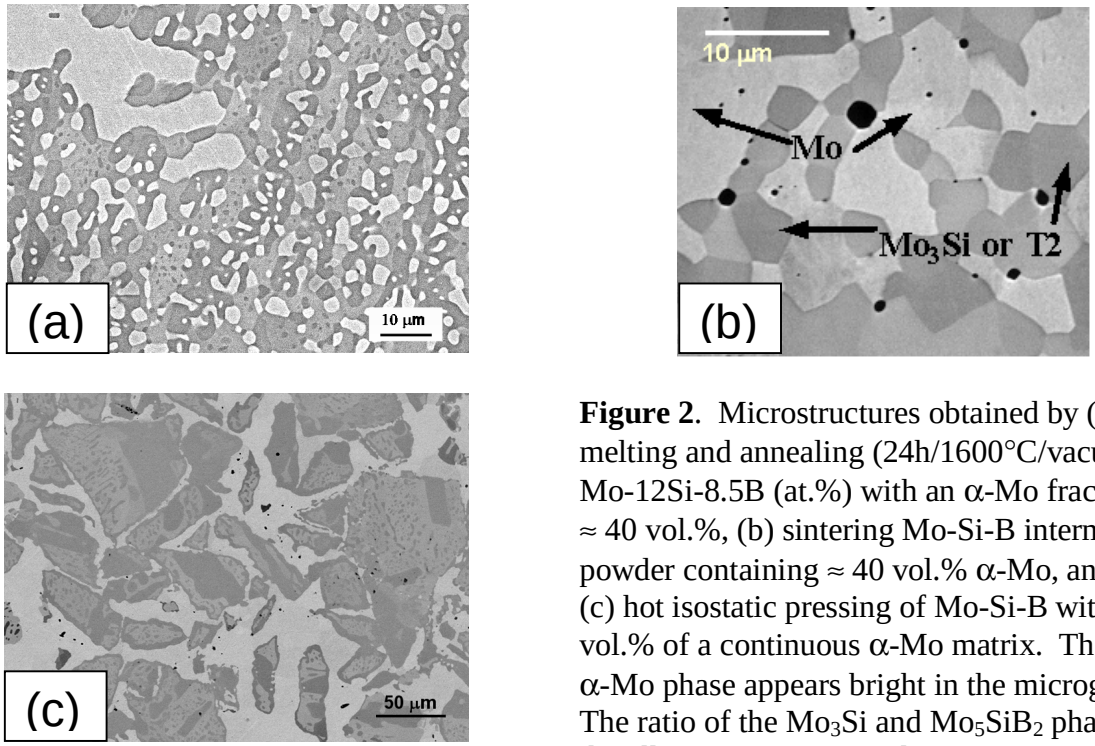

Figure 2. Microstructures obtained by (a) arc-melting and annealing (24h/1600°C/vacuum) Mo-12Si-8.5B (at.%) with an α-Mo fraction of ≈ 40 vol.%, (b) sintering Mo-Si-B intermetallic powder containing ≈ 40 vol.% α-Mo, and (c) hot isostatic pressing of Mo-Si-B with 34 vol.% of a continuous α-Mo matrix. The α-Mo phase appears bright in the micrographs. The ratio of the Mo_3Si and Mo_5SiB_2 phases in the alloys is approximately 50:50.

Oxidation resistance

As expected, the oxidation resistance at 1200°C decreases as the α-Mo volume fraction increases (Fig. 3). The initial rapid mass loss is characteristic of this class of materials and represents the creation of a volatile oxidation product of Mo, namely, MoO_3. Accordingly, the amount of initial mass loss increases with increasing α-Mo volume fraction. Following the initial mass loss, a plateau region of slowly changing mass is observed. At this point, more slowly growing condensed-phase reaction products (such as borosilicates) are presumably being formed.

Figure 4 shows the microstructures of two alloys with the same nominal compositions and α-Mo volume fractions (21%). The alloy on the left was fabricated from a mixture of Mo-Si-B and Mo powder, and the one on the right exclusively from Mo-Si-B powder. Since the α-Mo particles in

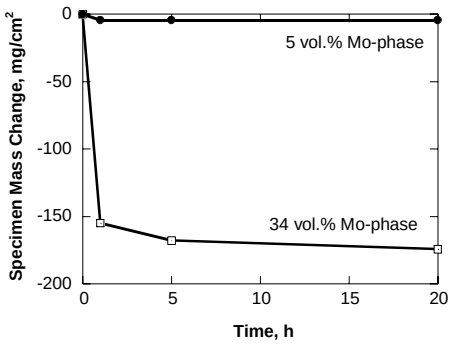

Figure 3. Specimen mass change vs. oxidation time at 1200°C in air for 1-h thermal cycles. The microstructure for the faster oxidizing alloy is shown in Fig. 3c. The other alloy was prepared similarly, but with a much lower α-Mo volume fraction.

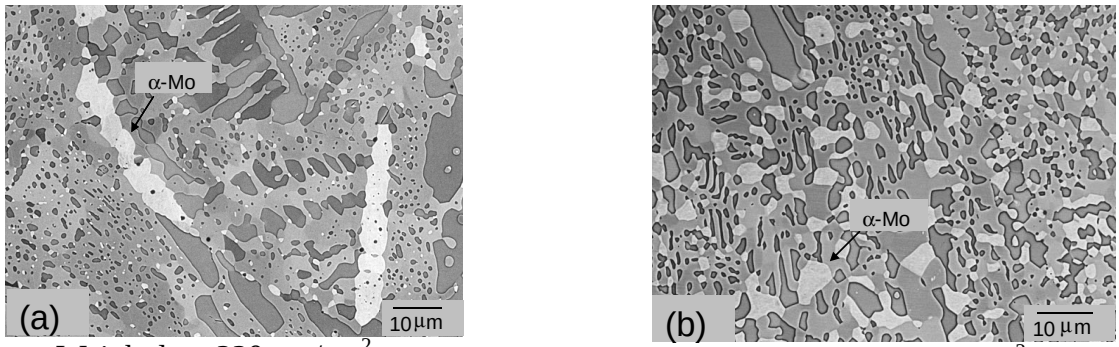

Weight loss 220 mg/cm^2 Weight loss 5.7 mg/cm^2

Figure 4. Micrographs of alloys with the same α-Mo volume fraction fabricated from a mixture of (a) Mo-Si-B and Mo powders and (b) exclusively from Mo-Si-B powder. The weight losses measured after 1 day at 1300°C in air show that the oxidation resistance depends strongly on the microstructural length scale.

the micrograph on the left are much coarser and elongated, as compared to the micrograph on the right, the oxidation rate is much higher. Therefore, in order to maximize the oxidation resistance the α-Mo volume fraction needs to be minimized and the α-Mo should occur in the form of small, individual particles.

Fracture toughness

Figure 5 illustrates the dramatic influence of the α-Mo volume fraction and topology on the room temperature fracture toughness. For 21 vol.% of a fine, particulate α-Mo phase, see Fig. 4b, the value of the fracture toughness is only 4.1 MPa m$^{1/2}$ [11]. Higher volume fractions increase the fracture toughness significantly. By changing the topology of the Mo-phase from one consisting of isolated particles to one consisting of a continuous binder phase, the toughening α-Mo phase is more efficiently used since the cracks cannot avoid the α-Mo. This is qualitatively illustrated in Fig. 5: the alloy with 34 vol.% of continuous α-Mo phase (see also Fig. 2c) exhibits a higher value of the fracture toughness, as well as a rising crack-growth resistance ("R-curve behavior") as compared to the cast alloy containing ≈ 40 vol.% of discontinuous α-Mo, see Fig. 2a [10]. Qualitatively, the continuous α-Mo phase, as compared to isolated particles, is more effective in promoting crack trapping; moreover, the larger α-Mo particles tend to remain unbroken in the crack wake and hence induce ductile-phase bridging. This means that a larger microstructural scale of the α-Mo phase tends to improve the fracture toughness.

Creep strength

The creep strength of Mo-Si-B alloys depends on the α-Mo volume fraction as well as the topology and length scale of the microstructure [13]. Figure 6 illustrates these dependencies. A low α-Mo volume fraction (21%) results in high creep strength. The presence of a continuous α-Mo phase tends to weaken the material, presumably because the sliding of individual Mo_3Si/Mo_5SiB_2 particles past each other is accommodated by the easily deformed α-Mo phase. Also, in general

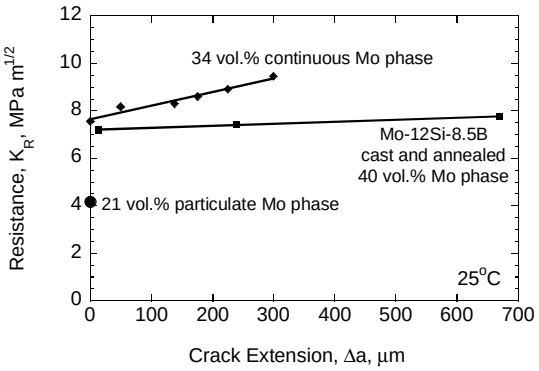

Figure 5. Fracture toughness of Mo-Si-B alloys as a function of α-Mo volume fraction as well as microstructural scale and topology.

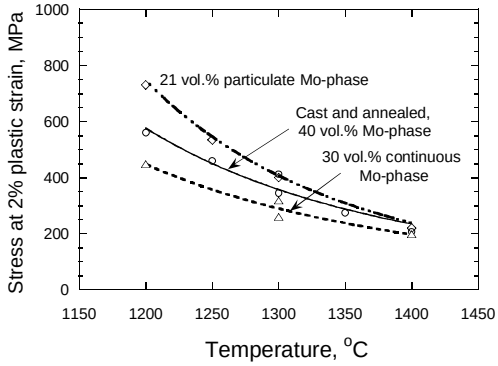

Figure 6. The creep strength of Mo-Si-B alloys depends on the α-Mo volume fraction and the topology of the microstructure.

coarse microstructures are preferred over fine microstructures because of the presence of fewer high-diffusivity paths such as grain and interphase boundaries.

SUMMARY AND CONCLUSIONS

Individually, some degree of oxidation resistance, fracture toughness, and creep strength of Mo-Si-B alloys can be obtained. However, it is presently not possible to obtain all these properties simultaneously. Essentially, the requirements for high fracture toughness run opposite to those for good oxidation and creep resistance as illustrated in Fig. 7. It will be difficult to improve the fracture toughness of the intermetallic phases Mo_3Si and Mo_5SiB_2. The α-Mo phase, with its simple bcc crystal structure, is more amenable to manipulation of its properties. Future work on Mo-Mo_3Si-Mo_5SiB_2 alloys should therefore concentrate on manipulation of the α-Mo phase in terms of obtaining improved ductility, fracture toughness, and oxidation resistance.

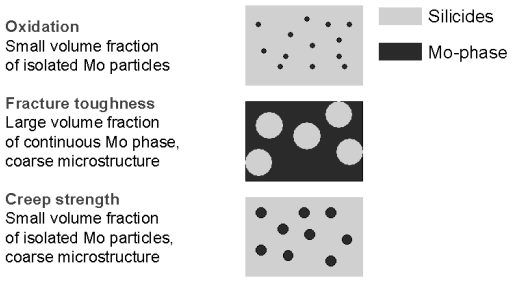

Figure 7. Schematic illustration of competing requirements for optimizing the oxidation resistance, fracture toughness, and creep strength of Mo-Mo_3Si-Mo_5SiB_2 alloys.

ACKNOWLEDGEMENTS

This work was sponsored by the Office of Fossil Energy, Advanced Research Materials (ARM) Program, and the Office of Basic Energy Sciences, Division of Materials Sciences and Engineering, U.S. Department of Energy (DOE), under contracts DE-AC05-00OR22725 with Oak Ridge National Laboratory managed by UT-Battelle, LLC, and No. DE-AC03-76SF00098 with the Lawrence Berkeley National Laboratory, and by the DOE National Energy Technology Laboratory under Field Work Proposal number AL-00-360-011. Ames Laboratory is operated for DOE by Iowa State University under contract No. W-7405-ENG-82. This work was part of the multi-National Laboratory program on "Design and Synthesis of Ultrahigh-Temperature Intermetallics" within the DOE Center for Excellence and Processing of Advanced Materials.

REFERENCES

1. M. K. Meyer, M. J. Kramer, and M. Akinc, Intermetallics 4 (1996) 273-281.
2. M. Akinc, M. K. Meyer, M. J. Kramer, A. J. Thom, J. J. Huebsch, and B. Cook, Intermetallics A261 (1999) 16-23.
3. M. K. Meyer, A. J. Thom, and M. Akinc, Intermetallics 7 (1999) 153-162.
4. D. M. Berczik, United States Patent 5,595,616 (1997), "Method for enhancing the oxidation resistance of a molybdenum alloy, and a method of making a molybdenum alloy."
5. D. M. Berczik, United States Patent 5,693,156 (1997), "Oxidation Resistant Molybdenum Alloys."
6. R. Raj and L. R. Thompson, Acta Metall. Mater. 42 (1994) 4135-4142.
7. J. H. Schneibel, M. J. Kramer, Ö. Ünal, and R. N. Wright, Intermetallics 9 (2001) 25-31.
8. J. H. Schneibel, M. J. Kramer, and D. S. Easton, Scr. Mater. 46[3] (2002) pp. 217-221.
9. B. A. Pint, P. F. Tortorelli, and I. G. Wright, pp. 111-32 in "Cyclic Oxidation Testing of High Temperature Materials," M. Schütze and W. J. Quadakkers (eds.), European Federation of Corrosion Publication 27, IOM Communications, London, 1999.
10. H. Choe, D. Chen, J. H. Schneibel, and R. O. Ritchie, Intermetallics, 9[4] (2001) 319-329.
11. H. Choe, J. H. Schneibel, and R. O. Ritchie, accepted for publication, Metall. Mater. Trans. A, 2003.
12. J. H. Schneibel and H. T. Lin, Materials at High Temperatures 19[1] (2002) 25-28.
13. J. H. Schneibel, D. S. Easton, H. Choe, and R. O. Ritchie, in "Structural Intermetallics, Third International Symposium," K. J. Hemker and D. M. Dimiduk, eds., TMS, Warrendale, PA, 2001, pp. 801-809.